

# Functional Connectivity Measures in Memory Networks Using Independent Component Analysis

Catarina Saiote Ferreira Leite

## Abstract

Memory function often appears to be compromised in several neurological pathologies and has been the subject of several studies within the field of neurosciences. The objective of this work was to explore methods for the analysis of functional connectivity of functional magnetic resonance imaging (fMRI) data, assessed by independent component analysis (ICA). Analysis was carried out using data from a previous study (Figueiredo et al. 2008) of memory function in normal subjects and patients with medial temporal lobe epilepsy and right hippocampal sclerosis. In order to do so, three different group ICA approaches were tested: tensorial group probabilistic ICA (PICA), group PICA with temporal concatenation approach and group ICA with temporal concatenation. Component sorting methods were developed and tested to assist in the selection of the components of interest. Overall, the tested ICA approaches yielded similar results with comparable networks, although, in general, the tensorial approach proved better in the detection of group differences, between normal controls and patients or between younger and older subjects.

**Keywords:** memory networks, fMRI, functional connectivity, independent component analysis.

## 1. Introduction

In today's neurosciences studies, data from several modalities is available. Functional magnetic resonance imaging (fMRI) is a widespread and valuable tool, which allows the study of the entire brain simultaneously. The most commonly used type of contrast in fMRI is the blood-oxygen-level-dependent (BOLD) signal, which depends on the balance between the consumption and supply of oxygen (Ogawa and Lee 1990). The BOLD signal is often compared to the neuronal activity in terms of the haemodynamic response function (HRF): the BOLD response to a stimulus of short duration, the temporal impulse response function.

Several methods have been developed to analyze fMRI data. These can be divided into model-free (data-driven) and model-based methods. The general linear model (GLM) is a widely used model-based method to analyse fMRI data. It describes the observed data as a linear combination of model functions, plus a noise term. For fMRI data this model is typically presented as follows:

$$X = G\beta + e \quad (1)$$

where  $X$  is the matrix containing the experimental data,  $G$  is called the design matrix in which the expected model functions are specified. The matrix  $\beta$  is the parameter

matrix, which contains the parameter weights that indicate how much each model effect contributes to the observed data (Figure 1a). The noise term is represented by  $e$ . (Worsley and Friston 1995).

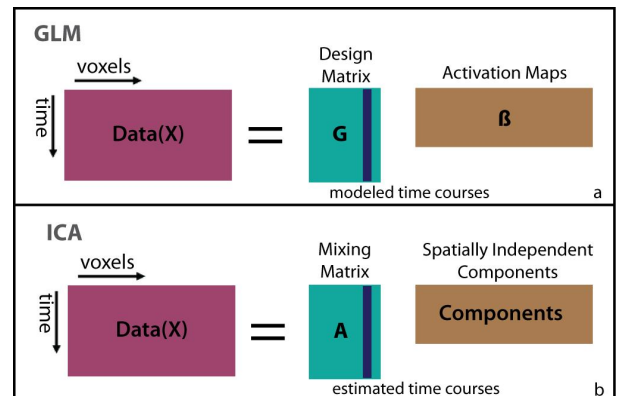


**Figure 1.** (a) In the GLM approach, a design matrix is constructed with the expected model effects and the estimated weight parameters yield spatial maps; (b) ICA estimates the time courses while searching for spatially independent components.

Although the GLM is the dominant tool for the analysis of fMRI data, conclusions are drawn assuming a given model, and there is no guaranty that the model itself is appropriate. In addition, the method makes certain assumptions that may cause limitations in the conclusions withdrawn (Huettel et al. 2004). Situations

exist in which there is no knowledge of an appropriate model and alternative approaches, such as data-driven methods like independent component analysis (ICA) (Figure 1b), have thus been developed.

ICA is a data analysis and signal processing method used to estimate unknown source signals from a signal where they have been mixed together by an unknown mixing process. ICA has several applications, one of them being to separate sources of brain activity either from electro-encephalography (EEG), magneto-encephalography (MEG) or fMRI data (Hyvärinen and Oja 2000).

According to the general ICA model for fMRI data (McKeown et al. 1998), the observed data matrix is generated by mixing the source signals or components. These are latent variables, since they cannot be observed directly, and assumed to be statistically independent and non-Gaussian. The mixing matrix is also unknown, and it is precisely the goal of ICA to estimate it, as well as the sources or independent components. Once the mixing matrix is estimated, it is possible to obtain the independent components by computing its inverse. Each spatial map is associated to a time-course contained in the associate column of the mixing matrix. A number of algorithms have been developed (Calhoun et al. 2009). The Infomax (Bell and Sejnowski 1995) and the FastICA (Hyvärinen 1999) algorithms are amongst the most commonly used and both perform well (Li et al. 2008).

A multitude of approaches has been suggested to generalize ICA to the analysis of group data. Some approaches try to perform ICA directly on the group data. Among these, temporal concatenation yields common spatial maps and subject-specific time-courses. Subject-specific results in one domain can be viewed as an advantage, since it allows straightforward comparison between subjects (Calhoun et al. 2001). On the other hand, when searching for a common representation for the entire group, both in the temporal and spatial domain, the tensorial approach (Beckmann and Smith 2005) seems more appropriate. ICA has been applied to the study of diverse aspects and may represent a source of complementary and relevant findings in the study of memory function (Kincses et al. 2008; Ranganath et al. 2005), networks in epilepsy or Alzheimer's Disease (AD) (Bai et al. 2009; Rombouts et

al. 2009; Voets et al. 2009), and resting state networks (De Luca et al. 2006; Wang et al. 2006).

The subject of brain connectivity analysis is the conjoint activity of different brain regions: how they connect and interact with each other in order to perform a cognitive function. (Li et al. 2008; Ramnani et al. 2002). When connectivity is studied from the point of view of the temporal correlation between the activity of different brain regions, regardless of its anatomical basis, it is classified as functional connectivity. (Li et al. 2008; Ramnani et al. 2004).

The study of functional connectivity can be carried out with model-based or data-driven methods. Model-based methods rely on prior knowledge or experience to select regions of interest (ROIs) and then search for other regions connected to these by using some metric of functional connectivity, such as cross-correlation, coherence analysis and statistical parametric mapping (using GLM) (Li et al. 2008). Data-driven methods can be based on clustering analysis or decomposition techniques (Li et al. 2008). The latter include principal component analysis (PCA), singular value decomposition (SVD) and independent component analysis (ICA). (Calhoun et al. 2009; Li et al. 2008; Rogers et al. 2007).

Several brain structures are known to play a role in episodic memory processes, such as the medial temporal lobe (MTL) and the prefrontal cortex (Kandell et al. 2000; Desgranges et al. 1998). Studies of memory function have also been performed when investigating changes in functional connectivity caused by mild cognitive impairment (MCI) and AD (Bai et al. 2009; Wang et al. 2006) (Rombouts et al. 2009). It was also found that functional connectivity (measured with correlation based methods) between chosen seed regions related to the task and other brain areas was a robust predictor of encoding success (Ranganath et al. 2005).

The main aim of this work was to explore methods for the analysis of functional connectivity. For this purpose, connectivity analyses were performed on memory networks, using ICA to search for components of interest and group differences. Three approaches of group ICA were compared. A set of criteria were defined to select components of interest from all the estimated sources.

## 2. Methods

The fMRI data used here was previously collected for a study of memory function (Figueiredo et al. 2008).

### 2.1. Subjects

Data were collected from a group of 20 healthy volunteers (CTRL), including 10 young (CTRL-Y) and 10 older adults (CTRL-O), and a group of 12 patients diagnosed with medial temporal lobe epilepsy (TLE) with right hippocampal sclerosis (RTLE). All patients had active temporal lobe epilepsy with typical complex partial seizures and were on antiepileptic drug treatment. All subjects were right-handed and had normal or corrected to normal vision. Informed consent was obtained from each subject according to guidelines approved by our institutional ethical committee. Exclusion criteria for both patients and controls were: major depression, dementia, and other neuropsychiatric disorders. Subgroups were selected of 10 normal subjects (CTRL-M) and 10 patients (RTLE-M) matched for age and behavioural performance. This was assessed by recognition scores and average response times. Although education and gender may have an effect in memory function, the fact that the two groups have matched behavioural performance should control for such effects. For technical reasons, the data from the Verbal task of one of the older controls had to be excluded from the study.

Different sub-divisions of subjects into groups were considered in the various analyses approaches described below: *All\_subj* – including all the subjects divided into controls (CTRL;  $n = 20$ ) and patients (RTLE;  $n = 12$ ); *All\_subj\_age* – subjects were subdivided into: younger normal subjects (CTRL-Y;  $n = 10$ ), older normal subjects (CTRL-O;  $n = 10$ ) and patients (RTLE;  $n = 12$ ); *Matched\_grps* – the subgroups of controls (CTRL-M;  $n = 10$ ) and patients (RTLE-M;  $n = 10$ ) matched for age and performance were considered; *Matched\_grps\_perf* – the sub-group of patients was further divided according to performance: controls (CTRL-M;  $n = 10$ ), patients with high performance (RTLE-H;  $n = 5$ ) and patients with low performance (RTLE-L;  $n = 5$ ).

### 2.2. Memory Paradigm

The subjects performed a Visual memory-encoding and a Verbal memory-encoding paradigm (Figueiredo et al. 2008). Each paradigm consisted of 10 cycles of one task block and one control block. Each task block lasted 18 s

during which 3 pairs of drawing/rotated drawing (Visual) or word/pseudoword (Verbal) were presented. Each block of 3 pairs was alternated with a control task of equal duration. In the visual task, subjects were instructed to select the drawing aligned with the vertical or horizontal axis, whereas the verbal task consisted of identification of the real word. During the control task subjects were asked to identify the position of a black square (left or right). Each task consisted of 10 cycles of encoding task followed by control task. A recognition task followed approximately 10 min after encoding. Subjects were shown the 30 previously studied targets pseudo-randomly intermixed with 30 novel foils, for each material type, and were asked to make old/new judgments on each item through a button press.

### 2.3. Image acquisition

The BOLD fMRI data were acquired on a 1.5 Tesla Philips Gyroscan Intera whole-body MRI system (Philips Medical System, Best, The Netherlands) using gradient-echo echo-planar-imaging (GE-EPI) with the following acquisition parameters: repetition time (TR) = 3000 ms, echo-time (TE) = 50 ms, and flip angle 90°. A total of ~30 axial slices were obtained with ~4 mm thickness, ~240 x 240 mm<sup>2</sup> field of view, and 64 x 64 acquisition matrix, yielding a voxel size of ~3.5 x 3.5 x 4.0 mm<sup>3</sup>. Each functional scan consisted of 120 volumes with a total duration of 360s (6min). To obtain T1-weighted structural images, a spoiled gradient recalled echo (SPGR) pulse sequence was used in the same session, with axial slices of 1 mm thickness, ~240 x 240 field of view and 256 x 256 acquisition matrix, yielding a reconstructed voxel of ~1 mm<sup>3</sup>.

### 2.4 fMRI analysis

For the analysis of fMRI data, specially developed software tools were used, in particular: FSL (FMRIB's Software Library, [www.fmrib.ox.ac.uk/fsl](http://www.fmrib.ox.ac.uk/fsl)) Version 4.12 and for ICA, the MELODIC (v3.09) and GIFT (v1.3g) tools were used.

#### 2.4.1 Pre-processing

Pre-processing of fMRI datasets from both tasks was carried out using FEAT (fMRI Expert Analysis Tool) Version 5.98, part of FSL and included: motion correction by co-registration of all volumes to a reference volume using MCFLIRT (Jenkinson et al. 2002); non-brain structures removal using BET (Brain

Extraction Tool) (Smith 2002); spatial smoothing using a Gaussian kernel of 5.0 mm or 8.0 mm FWHM (Full Width Half Maximum); grand-mean intensity normalisation of the entire 4D dataset by a single multiplicative factor; and high-pass temporal filtering (Gaussian-weighted least-squares straight line fitting, 50 s cutoff).

#### 2.4.2 GLM analysis

Data from each subject were entered in a (GLM) analysis with local autocorrelation correction using FMRIB's Improved Linear Model (FILM), to search for encoding-related activity changes (Woolrich et al. 2001). Regressors for each task consisted of a square function of width corresponding to the stimulus duration convolved with the canonical Gamma-variate haemodynamic response function (HRF). The first time derivative of the canonical HRF was also included in the model as a regressor. Also, six motion parameters (three of translational and three of rotational motion) were added as covariates of no interest. The parameter estimates (PE) were obtained by using a least squares algorithm. Linear contrasts of parameter estimates (COPE) between the visual and verbal encoding conditions and the control baseline were then calculated, yielding statistical maps of increased brain activity for each task and subject. Group analyses were carried out using FLAME (FMRIB's Local Analysis of Mixed Effects) - stage 1 (Beckmann et al. 2003; Woolrich et al. 2004), consisting on a mixed-effects (fixed and random effects) approach using Bayesian estimation techniques. Low-resolution functional images were registered to the corresponding high-resolution T1-weighted structural images of each subject. These were in turn registered to the Montreal Neurological Institute (MNI) template for a standard brain (Collins et al. 1994) with a resolution of  $2 \times 2 \times 2 \text{ mm}^3$ , using FMRIB's Linear Image Registration Tool (FLIRT) (Jenkinson et al. 2002; Jenkinson and Smith 2001). For each task, the individual normalized COPE images were then entered into a second-level statistical analyses and the mean group effects were identified by one sample t-tests for each group. Contrasts were defined for group/subgroup comparisons. Gaussian random fields (GRF) theory was used to accomplish maximum-height thresholding of the Z-score images at the significance level  $p = 0.05$ , corrected for multiple comparisons (Worsley 2001).

#### 2.4.3 Independent Component Analysis

Three different ICA implementations for group fMRI data were explored: *tensor-PICA* (Tensorial Probabilistic Independent Component Analysis) in MELODIC/FSL; *concat-PICA* (PICA with temporal concatenation) in MELODIC/FSL; *concat-ICA* (ICA with temporal concatenation) in GIFT toolbox.

##### *Single-subject PICA*

The original ICA model for fMRI data (McKeown et al. 1998) does not include a noise model, hence assuming that the estimated sources and the mixing matrix completely account for the observed data. In the probabilistic ICA (PICA) model (Beckmann and Smith 2004), the mixing matrix is allowed to be non-square and the data are assumed to be confounded by additive Gaussian noise. It can be defined as follows:

$$\mathbf{x}_i = \mathbf{A}\mathbf{s}_i + \boldsymbol{\mu} + \boldsymbol{\eta}_i \quad (2)$$

where  $\mathbf{x}_i$  stands for the  $p$ -dimensional column vector of individual measurements at  $i^{\text{th}}$  voxel,  $\mathbf{s}_i$  is the  $q$ -dimensional column vector of non-Gaussian source signals and  $\boldsymbol{\eta}_i$  represents Gaussian noise,  $\boldsymbol{\eta}_i \sim N(0, \sigma^2 \boldsymbol{\Sigma}_i)$ . It is assumed that  $q < p$ , that is, there are fewer source processes than observations in time. The vector  $\boldsymbol{\mu}$  denotes the mean of the observations  $\mathbf{x}_i$  where the index  $i$  is over the set of all voxel locations  $V$  and the matrix  $\mathbf{A}_{p \times q}$  is assumed to be of rank  $q$ . The goal is to find matrix  $\mathbf{W}$  such that

$$\hat{\mathbf{s}} = \mathbf{W}\mathbf{x} \quad (3)$$

is a good approximation to the true source signals  $\mathbf{s}$  (Beckmann and Smith 2004). The process of estimating  $\hat{\mathbf{s}}$  consists of three stages: (1) estimation of the number of components; (2) estimation of the independent components and noise; (3) evaluation of the statistical significance of the estimated sources. In the first step, probabilistic PCA (Tipping and Bishop 1999) is used to find a linear subspace containing the sources and a noise subspace orthogonal to the first. The estimation of the number of sources is a problem of model order selection. This can be inferred from the covariance matrix of the observations using a Bayesian framework to approximate the posterior distribution of model order (Minka 2000). In the second stage of the ICA process a fixed-point iteration algorithm (Hyvärinen 1999) is used to estimate the components. In the third step is the individual IC maps are converted into Z-statistic maps by

performing a division of the raw IC maps by the estimate of the voxel-wise noise standard deviation. After that, Gaussian mixture modelling of the probability density of the spatial map of Z-scores is used in order to find out which voxels are significantly activated, with an alternative-hypothesis testing approach (Beckmann and Smith 2004). This model is implemented as the MELODIC tool as part of FSL.

#### *Tensor-PICA (MELODIC)*

Tensorial Independent Component Analysis (*tensor-PICA*) is a technique that extends single-session PICA to higher dimensions as an approach to multi-subject or multisession fMRI data analysis with ICA. To allow comparison of voxel locations between subjects, individual data-sets must be registered to a common space (Beckmann and Smith 2005). Analyses with *tensor-PICA* were performed corresponding to each one of the GLM group analysis as implemented in MELODIC Version 3.09, part of FSL (FMRIB's Software Library, [www.fmrib.ox.ac.uk/fsl](http://www.fmrib.ox.ac.uk/fsl)). Besides the pre-processing steps mentioned in 2.4.1, the following were applied to the input data: masking of non-brain voxels and voxel-wise de-meaning of the data; normalisation of the voxel-wise variance.

The analysis follows the steps described for PICA. A GLM analysis was used to compare the estimates time-courses (one per component) with the task design. Additionally, the estimated relative amplitudes for each subject (*subject mode*) were used to search for significant changes between the groups defined for the described second-level model-based analyses. This was carried out for each component using a GLM approach.

#### *Concat-PICA (MELODIC)*

The PICA-based group approach with temporal concatenation requires the same pre-processing steps as *tensor-PICA*. Analyses were run for *All\_subj\_age* and *Matched\_grps* sets previously described. An initial data reduction step is performed by projecting each dataset onto a common PCA eigenbasis, calculated from the mean data covariance matrix. The resulting datasets are then temporally concatenated and follow the same steps delineated for PICA. As performed in the *tensor-PICA* analyses, the time-courses were compared with the task design, to find the components best related to the task. However, unlike the tensorial approach, *concat-PICA* estimates one time-course per subject for each

component. Therefore, the GLM analysis is performed using the best rank-1 approximation to the time-courses. The estimated responses in the *subject mode* were used to test for group differences as described for *tensor-PICA*.

#### *Concat-ICA (GIFT)*

The same pre-processed data were entered into analysis with the GIFT Matlab toolbox, using only the spatially smoothed data with a Gaussian kernel of FWHM = 5 mm (Calhoun et al. 2001). The number of sources was estimated using the Akaike's Information Criterion / Minimum Description Length criterion (Akaike 1974; Rissanen 1983) and this was applied to one subject, yielding less than 20 components. The number of components was fixed to the same number as obtained with MELODIC, that is, 20 for the Visual task including all the subjects and 19 for the Verbal task. The concatenated data were reduced to this dimension using PCA and then entered into the independent component estimation stage, where the Infomax algorithm (Bell and Sejnowski 1995) was used. Time-courses and spatial maps for each subject were obtained by multiplying the partition of the unmixing matrix that corresponds to each subject's data with the corresponding partition of the data. The mean and standard deviation of each component was then calculated across subjects as well as the corresponding *t*-maps (Calhoun et al. 2001). These were thresholded at a level of significance  $p = 0.05$ . The components' time-courses were compared to the GLM design using multiple correlation analysis.

#### *Component sorting*

As implemented in MELODIC, the median response amplitude across subjects was computed for each component and they were ordered in decreasing order of this value. To sort the components of interest obtained with *tensor-PICA* for further analysis, a group of criteria were thought of that would ensure the components were task-related and relevant across all the subjects. Thus, components should: (i) be significantly related to the GLM design ( $p = 0.05$ ); (ii) have positive response amplitude for all the subjects. Additionally, components clearly corresponding to motion artifacts were excluded by visual inspection. Once the components of interest were identified, they were used to perform another round of *tensor-PICA* analyses that might be more sensitive to group

differences. A script was written to create a mask derived from each of the components of interest, apply it to the pre-processed data of the corresponding task (*Visual* or *Verbal*) and run MELODIC. Each analysis was also carried out with reduction to the fixed number of 20 and 10 components.

### 3. Results

#### 3.1. GLM – Second-Level Analyses

Group analyses for all the subjects yielded no significant differences in activity between groups. These results are in accordance with those reported in a previous study using the same datasets (Figueiredo et al. 2008).

#### 3.2. ICA Analyses

All the ICA analysis yielded components showing activations in expected regions, considering the task, as well as components related to residual motion artifacts and other components harder to interpret. All the data were registered and transformed to MNI standard space and all images show the components overlaid on the MNI template for a standard brain (T1 contrast structural image with non-brain structures removed) with a resolution of  $2 \times 2 \times 2 \text{ mm}^3$ .

##### 3.2.1. *Tensor-PICA* results

Analyses carried out with spatial smoothing with a Gaussian kernel of FWHM = 5 mm yielded more components of interest. Therefore, in all subsequent results this parameter is fixed. The subject-mode revealed, for all analyses of the Visual Encoding data, four components of interest. As for the Verbal Encoding, the *All\_subj* analysis yielded two components of interest, while three components were obtained with each of the other analyses.

The components of interest obtained for the Visual task in the *All\_subj\_age* analysis are shown in Figure 2a. IC1 shows activations in the visual areas, including both the dorsal and ventral pathways. The network also includes deactivations (in blue-lightblue in Figure 2) that correspond a resting state network (RSN) described in the literature (De Luca et al. 2006). IC2 includes mainly Visual areas, as in IC1, but more extensively activated in the parietal cortex. IC3 is very similar to IC1 regarding the regions with positive values, differing in the regions where deactivations were identified. These include the

cuneus and precuneus, and other regions which form the RSN2. IC4 presents inferior and posterior regions in occipital cortex and deactivations in small frontal and parietal areas. The four described components' time-courses show significant correlation with the task at  $p < 0.00000$ . Corresponding results for the Verbal task are presented in Figure 2b. The first component is similar to IC1 described for the Visual task. In addition, it includes a lateralized region in the left frontal cortex including Broca's area. IC2 comprises regions on the inferior and middle occipital and temporal cortices, frontal pole and also in the left and right hippocampus and parahippocampal gyrus. IC3 consists of visual areas, and also regions in the lingual gyrus and temporal occipital fusiform cortex.

Regarding the other analyses performed (*All\_subj*, *Matched\_grps* and *Matched\_grps\_perf*), the obtained components are very similar, differing only in ordering and on the extension of the activation of some regions. Significant changes between groups for each component were assessed using a GLM approach on each subject's relative response amplitude across the subject domain. None of the *tensor-PICA* analysis yielded any component with significant (significance level  $p = 0.05$ ) changes between the defined groups either for the Visual as well as Verbal tasks. This is accordance with standard GLM second-level analysis.

##### 3.2.2. *Concat-PICA* results

The temporal concatenation approach was carried out in *All\_subj\_age* and *Matched\_grps* analyses. In *All\_subj\_age* only one component of interest, similar to IC1, was obtained (Figure 3a). It is, however, worth mentioning the fourth component identified in *All\_subj\_age* analysis. It comprises solely deactivations, corresponding to RSN2 and shows significant differences (Figure 3b and 3c) between the CTRL-Y and CTRL-O groups ( $p < 0.022$ ). Concerning the Verbal Encoding task, only the first component (similar to IC1) was of interest.

The analysis *Matched\_grps* yielded three components of interest for the Visual task and one for the Verbal task. The estimated components of interest are similar to others obtained in previous analyses. None of the components show significant group differences.

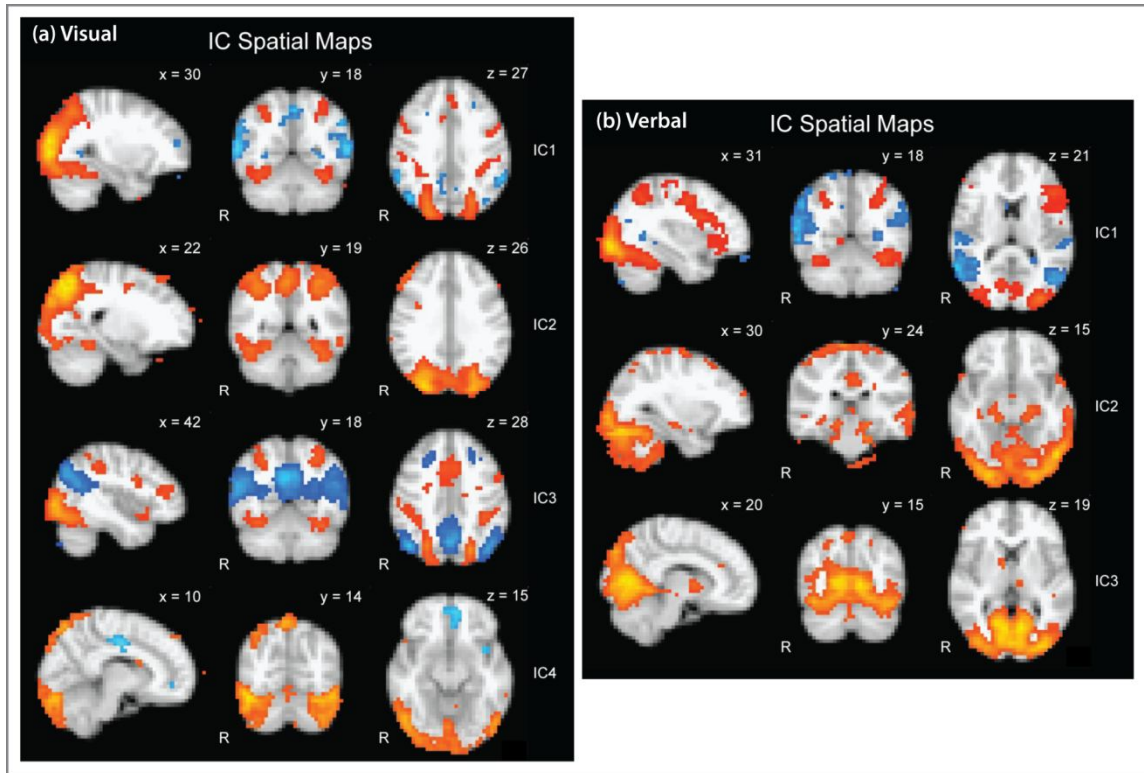


**Figure 2.** Components of interest for *tensor-PICA* analysis (FWHM = 5 mm) of Visual (a) and Verbal (b) Encoding tasks in *All\_subj\_age* analysis: spatial maps (alternative hypothesis threshold at  $p > 0.5$  for activation versus null) showing regions positively correlated with the task (red-yellow) and inversely correlated with the task (blue-lightblue).

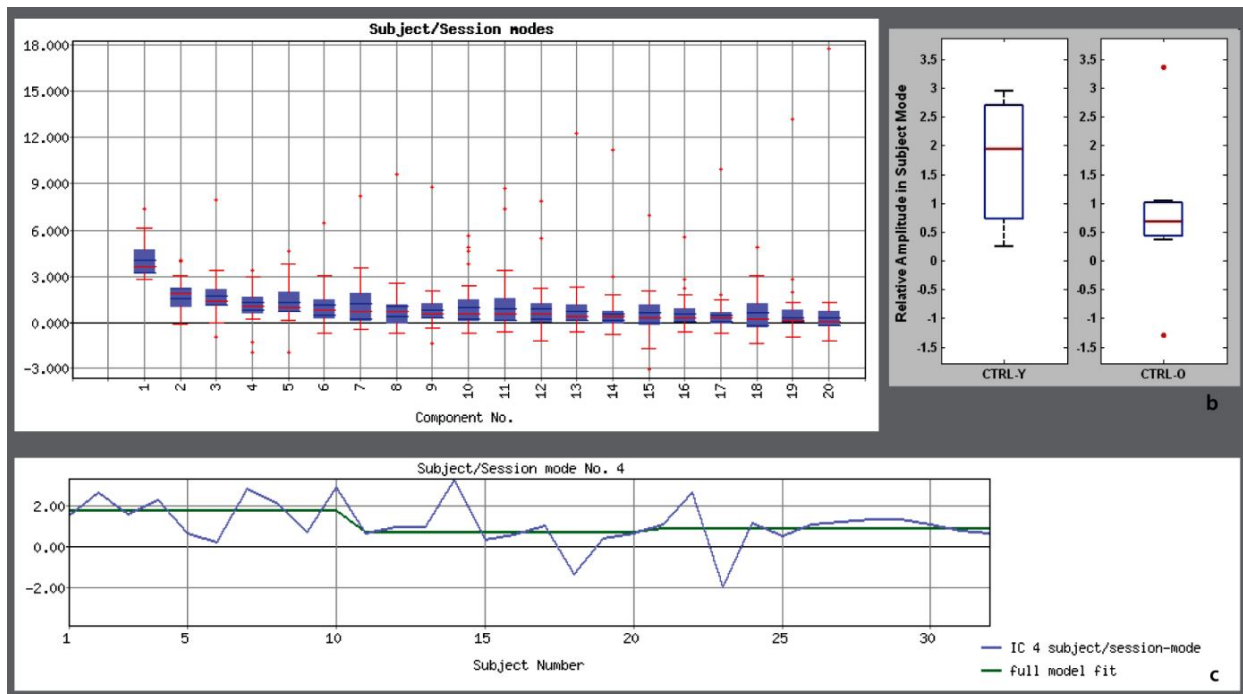


**Figure 3.** Subject modes for *All\_subj\_age* analysis of the Visual task using *concat-PICA* (FWHM = 5 mm): (a) Boxplots of the subject modes for the 20 components; (b) Boxplots for relative amplitude in subject mode in the first component, for subjects in CTRL-Y and CTRL-O groups; (c) comparison of the subject-specific value for the groups CTRL-Y (subjects 1-10), CTRL-O (subjects 11-20) and RTLE (subjects 21-32).



### 3.2.3. Concat-ICA results

The *concat-ICA* analyses yielded components comparable to those obtained with MELODIC. The components were ordered by decreasing order of correlation with the task assessed by multiple regression analysis between the GLM design and each component's time course. The components obtained for the Verbal task analysis are shown in Figure 3.

### 3.2.4. Component Sorting

When *tensor-PICA* analysis was performed using a mask to select the voxels corresponding to one of the previously estimated components of interest from *All\_subj\_age* analysis, significant results were obtained regarding group comparisons (Table1). For the *concat-ICA* analyses, components were ordered by performing multiple regression analysis between the IC time-courses and the task design. Only components with  $r > 0.05$  were considered.

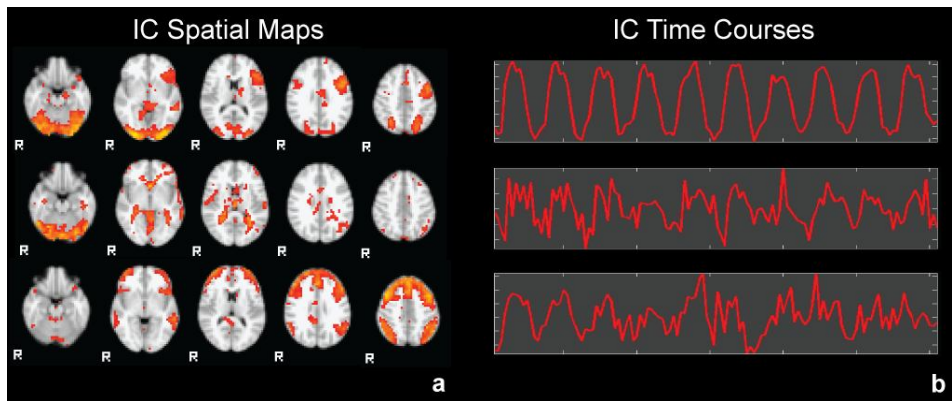


**Figure 4.** Estimated components in the *All\_subj\_age* analysis in *concat-ICA* (FWHM = 5 mm) for the Verbal task. Components shown are ordered by decreasing value of correlation to the task design (IC1 -  $r = 0.3121$ ; IC2 -  $r = 0.0913$ ;  $r = 0.0634$ ): (a) spatial maps (axial views at  $z = -20$  mm,  $-4$  mm,  $12$  mm,  $28$  mm and  $44$  mm) thresholded at  $p = 0.05$  ( $t = 1.697$ ,  $df = 30$ ); (b) time courses for each component.

**Table 1.** Estimated ICs that showed significant differences between groups, in analyses performed with prior masking to select the regions defined by previously estimated components.

Group Comparison $p < 0.05$	Visual Encoding				Verbal Encoding			
	CTRL-Y>CTRL-O			CTRL-Y>RTLE CTRL-O>RTLE	CTRL-Y>CTRL-O			CTRL-Y>RTLE CTRL-O>RTLE
Mask	#1	#2	#3	#1	#1	#2	#3	#1
Automatic Dimensionality Estimation	IC1	IC6, IC7, IC8	IC8	IC9	IC4, IC7	IC4	IC5, IC7	IC13
20 Components	IC3	IC2, IC4	IC2, IC5, IC7	IC7	IC2	-	IC4	-
10 Components	-	IC2, IC4	IC3	-	-	IC2	IC2	-

## 4. Discussion

In all the analyses performed it was possible to find components comprising brain regions where activations were indeed expected, considering the task performed.

In general, the analyses using *tensor-PICA* yielded interesting results in the spatial, temporal and subject domains. Regarding the pre-processing parameters, it can be concluded that performing spatial-smoothing with a Gaussian kernel of smaller FWHM (5 mm) yielded a

higher number of components and allowed a better separation of source processes of interest.

When *concat-PICA* results are compared to those obtained with *tensor-PICA*, it is possible to observe that fewer components can be classified as components of interest according to the specified criterion. The datasets are the result of a block-design memory task, and consequently all subjects' time-courses are expected to be similar. In this scenario, the tensorial approach is, in



principle, the one recommended (Beckmann and Smith 2005; Calhoun et al. 2009).

In what regards the components yielded by the *concat-ICA* analyses, they are similar to those obtained using PICA approaches. The assessment of statistical significance after the ICA decomposition within the GIFT implementation is performed differently from the approaches using PICA. Therefore, care must be taken when comparing the results of the two approaches. However, it is possible to say that using a significance level of  $p < 0.05$  to threshold the estimated spatial maps, yielded components with comparable extent of activation in most regions, in comparison with the alternative test performed within the PICA framework of  $p > 0.5$  (above 50% chance of not belonging to the background noise).

All of the ICA approaches used in this work yielded some components with deactivations. Among these, two patterns that correspond to resting state networks (RSNs) previously identified in the literature, namely RSN2 (for the visual task) and RSN5 (both tasks) (De Luca et al. 2006). It has been suggested that RSN2 is involved in a functional network related to processes of internal monitoring and states of consciousness. The areas belonging to RSN5 resemble the ventral visual pathway. (De Luca et al. 2006) In a number of studies using ICA, RSNs were identified either while subjects performed a task or during rest. Since this technique is able to differentiate these patterns from those related to cardio-respiratory motion and other noise sources, it is possible that RSNs may result from some sort of neuronal activity. They may be useful as a marker for functional alterations, since some studies have observed changes when comparing RSNs of normal subjects and patients (De Luca et al. 2006; Kincses et al. 2008; Rombouts et al. 2009)

Considering the criteria defined to select the components, it can be concluded that the *tensor-PICA* yielded more components of interest, mainly due to their consistency across subjects. These components were further investigated by performing masking of brain voxels prior to the ICA decomposition. This allowed the identification of smaller networks showing significant group differences, leading to the conclusion that this step increased the sensitivity of the group comparison analysis, as expected. Some of the obtained networks showed a significant age effect within normal subjects. Also, differences between normal subjects and patients

in a network including the occipital pole and lateral occipital cortex, and deactivations in the middle temporal gyrus (RSN5).

Overall, it can be said that, being a data-driven approach, ICA is of particular relevance in the analysis of data from disease studies, where there is higher inter-subject variability. Model-free analysis is of particular interest in the analysis of studies of disease or aging, since it has been discussed that this subjects' HRF can deviate significantly from the canonical function used in most analyses and model-based techniques can thus be compromised (Rombouts et al. 2009). Group ICA analyses can thus be used to point out changes in brain networks in diseases, such as epilepsy or AD that would otherwise be unnoticed or detect only at a later stage.

Regarding the component sorting method, we have explored the potential of using the components identified in a first ICA decomposition as masks for a second ICA. We found that this procedure improved the sensitivity for the detection of connectivity group differences. However, it is necessary to test the sorting criteria and the masking step in datasets from different studies, if possible with increased number of subjects, in order to be able to conclude about the improvements in the statistical significance of group differences. Additionally, the masking step was not applied to a temporal concatenation analysis, which would be of importance to better compare the two approaches. In what regards the *concat-ICA* analyses, it is possible to conclude that the identified components are similar, but any other comparisons would be premature. It would be advisable to use the time-courses estimated to test for significant group differences. In the future, it would also be interesting to select the components of interest by comparing them with anatomical masks of regions where activation (or deactivation) is expected or desired.

Finally, the connectivity study here presented could be further completed by performing effective connectivity analyses based on the results obtained, using methods such as Dynamic Causal Modelling (DCM) (Friston et al. 2003) or Granger Causality (Rogers et al. 2007). In particular, these could be used to evaluate the effective connectivity between the MTL and visual cortex, and also between regions in the prefrontal cortex that showed activations by measuring the relative strength as well as the direction of the connections between the activated or deactivated areas.

## References

- Akaike, H. (1974). "A New Look at Statistical Model Identification." *IEEE Trans Automatic Control*, 19, 716-723.
- Bai, F., Zhang, Z., Watson, D. R., Yu, H., Shi, Y., Yuan, Y., Zang, Y., Zhu, C., and Qian, Y. (2009). "Abnormal Functional Connectivity of Hippocampus During Episodic Memory Retrieval Processing Network in Amnesic Mild Cognitive Impairment." *Biological Psychiatry*, 65, 951-958.
- Beckmann, C. F., Jenkinson, M., and Smith, S. M. (2003). "General Multi-Level Linear Modelling for Group Analysis in fMRI." *NeuroImage*, 20, 1052-1063.
- Beckmann, C. F., and Smith, S. M. (2004). "Probabilistic Independent Component Analysis for Functional Magnetic Resonance Imaging." *IEEE Transactions on Medical Imaging*, 23(2), 137-152.
- Beckmann, C. F., and Smith, S. M. (2005). "Tensorial Extensions of Independent Component Analysis for Multisubject fMRI Analysis." *NeuroImage*, 25(1), 294-311.
- Bell, A., and Sejnowski, T. J. (1995). "An Information-Maximization Approach to Blind Separation and Blind Deconvolution." *Neural Comput*, 7(6), 1129-1159.
- Calhoun, V. D., Adali, T., Pearlson, G. D., and Pekar, J. J. (2001). "A Method for Making Group Inferences from Functional MRI Data Using Independent Component Analysis." *Human Brain Mapping*, 14, 140-151.
- Calhoun, V. D., Liu, J., and Adali, T. (2009). "A Review of Group ICA for fMRI Data and ICA for Joint Inference of Imaging, Genetic, and ERP Data." *NeuroImage*, 45(1 Suppl), S163-S172.
- Collins, D. L., Neelin, P., Peters, T. M., and Evans, A. C. (1994). "Automatic 3D Inter-Subject Registration of MR Volumetric Data in Standardized Talairach Space." *J Comput Assist Tomogr*, 18, 192-205.
- De Luca, M., Beckmann, C. F., De Stefano, N., Matthews, P. M., and Smith, S. M. (2006). "fMRI Resting State Networks Define Distinct Modes of Long-Distance Interactions in the Human Brain." *NeuroImage*, 29, 1359-1367.
- Desgranges, B., Baron, J., and Eustache, F. (1998). "The Functional Neuroanatomy of Episodic Memory: The Role of the Frontal Lobes, the Hippocampal Formation, and Other Areas." *NeuroImage*, 8, 198-213.
- Figueiredo, P., Santana, I., Teixeira, J., Cunha, C., Machado, E., Sales, F., Almeida, E., and Castelo-Branco, M. (2008). "Adaptive Visual Memory Reorganization in Right Medial Temporal Lobe Epilepsy." *Epilepsia*, 49(8), 1395-1408.
- Friston, K. J., Harrison, L., and Penny, W. (2003). "Dynamic Causal Modelling." *NeuroImage*, 19, 1273-1302.
- Huettel, S. A., Song, A. W., and McCarthy, G. (2004). *Functional Magnetic Resonance Imaging*, Sinauer Associates, Inc.
- Hyvärinen, A. (1999). "Fast and robust fixed-point algorithms for independent component analysis." *IEEE Transactions on Neural Networks*, 10(3), 626-634.
- Hyvärinen, A., and Oja, E. (2000). "Independent Component Analysis: Algorithms and Applications." *Neural Networks*, 13(4-5), 411-430.
- Jenkinson, M., Bannister, P., Brady, M., and Smith, S. M. (2002). "Improved Optimisation for the Robust and Accurate Linear Registration and Motion Correction of Brain Images." *NeuroImage*, 17(2), 825-841.
- Jenkinson, M., and Smith, S. M. (2001). "A Global Optimisation Method for Robust Affine Registration of Brain Images." *Medical Image Analysis*, 5(2), 143-156.
- Kandell, E. R., Schwartz, J. H., and Jessel, T. M. (2000). *Principles of Neural Science*, McGraw-Hill.
- Kincses, Z. T., Johansen-Berg, H., Tomassini, V., Bosnell, R., Matthews, P. M., and Beckmann, C. F. (2008). "Model-Free Characterization of Brain Functional Networks for Motor Sequence Learning Using fMRI." *NeuroImage*, 39, 1950-1958.
- Li, K., Guo, L., Nie, J., Li, G., and Liu, T. (2008). "Review of Methods for Functional Connectivity Detection Using fMRI." *Computerized Medical Imaging and Graphics*, 33, 131-139.
- McKeown, M. J., Makeig, S., Brown, G., Jung, T., Kindermann, S. S., Bell, A., and Sejnowski, T. J. (1998). "Analysis of fMRI Data by Blind Separation Into Independent Spatial Components." *Human Brain Mapping*, 6, 160-188.
- Minka, T. (2000). "Automatic Choice of Dimensionality for PCA." *Technical Report 514*. MIT Media Lab Vision and Modeling Group.
- Ogawa, S., and Lee, T. M. (1990). "Magnetic Resonance Imaging of Blood Vessels at High Fields: In Vivo and In Vitro Measurements and Image Simulation." *Magn. Reson. Med.*, 16(1), 9-18.
- Ramnani, N., Behrens, T. E. J., Penny, W., and Matthews, P. M. (2004). "New Approaches for Exploring Anatomical and Functional Connectivity in the Human Brain." *Biological Psychiatry*, 56, 613-619.
- Ramnani, N., Lee, L., Mechelli, A., Phillips, C., Roebroeck, A., and Formisano, E. (2002). "Exploring Brain Connectivity: a New Frontier in Systems Neurosciences." *Trends in Neurosciences*, 25(10).
- Ranganath, C., Heller, A., Cohen, M. X., Brozinsky, C. J., and Rissman, J. (2005). "Functional Connectivity with the Hippocampus During Successful Memory Formation." *Hippocampus*, 15, 997-1005.
- Rissanen, J. (1983). "A Universal Prior for Integers and Estimation by Minimum Description Length." *Ann Statistics*, 11, 416-431.
- Rogers, B. P., Morgan, V. L., Newton, A. T., and Gore, J. C. (2007). "Assessing Functional Connectivity in the Human Brain by fMRI." *Magnetic Resonance Imaging*, 25(10), 1347-1357.
- Rombouts, S. A., Damoiseaux, J. S., Goekoop, R., Barkhof, F. S., P, Smith, S. M., and Beckmann, C. F. (2009). "Model-Free Group Analysis Shows Altered BOLD fMRI Networks in Dementia." *Human Brain Mapping*, 30, 256-266.
- Smith, S. M. (2002). "Fast Robust Automated Brain Extraction." *Human Brain Mapping*, 17(3), 143-155.
- Tipping, M. E., and Bishop, C. M. (1999). "Probabilistic Principal Component Analysis." *J Royal Statistical Society B*, 61(3).
- Voets, N. L., Adcock, J. E., Stacey, R., Hart, Y., Carpenter, K., Matthews, P. M., and Beckmann, C. F. (2009). "Functional and Structural Changes in the Memory Network Associated With Left Temporal Lobe Epilepsy." *Human Brain Mapping*.
- Wang, L., Zang, Y., He, Y., Liang, M., Zhang, X., Tian, L., Wu, T., Jiang, T., and Li, K. (2006). "Changes in Hippocampal Connectivity in the Early Stages of Alzheimer's Disease: Evidence from Resting State fMRI." *NeuroImage*, 31, 496-504.
- Woolrich, M. W., Behrens, T. E. J., Beckmann, C. F., Jenkinson, M., and Smith, S. M. (2004). "Multi-Level Linear Modelling for fMRI Group Analysis Using Bayesian Inference." *NeuroImage*, 21(4), 1732-1747.
- Woolrich, M. W., Ripley, B. D., Brady, M., and Smith, S. M. (2001). "Temporal Autocorrelation in Univariate Linear Modelling of fMRI Data." *NeuroImage*, 14(6), 1370-1386.
- Worsley, K. J. (2001). "Statistical analysis of activation images. Ch 14." *Functional MRI: An Introduction to Methods*, P. Jezzard, P. M. Matthews, and S. M. Smith, eds., Oxford University Press.
- Worsley, K. J., and Friston, K. J. (1995). "Analysis of fMRI Time-Series Revisited - Again." *NeuroImage*, 2, 173-181.